Nonlinear nanochannels for room temperature terahertz heterodyne detection



2013 Semicond. Sci. Technol. 28 125024

(http://iopscience.iop.org/0268-1242/28/12/125024)

Semicond. Sci. Technol. **28** (2013) 125024 (6pp) doi:10.1088/0268-1242/28/12/125024

# Nonlinear nanochannels for room temperature terahertz heterodyne detection

**Jeremie Torres[1], Philippe Nouvel[1], Alexandre Penot[1], Luca Varani[1], Paul Sangaré[2], Bertrand Grimbert[2], Marc Faucher[2], Guillaume Ducournau[2], Christophe Gaquière[2], Ignacio Iñiguez-de-la-Torre[3], Javier Mateos[3] and Tomas Gonzalez[3]**

[1] Institut d'Electronique du Sud, CNRS UMR F-5214, TeraLab, Université Montpellier 2, France
[2] Institut d'Électronique de Microélectronique et de Nanotechnologie, CNRS UMR F-8520, Université de Lille 1, France
[3] Departamento de Fisica Aplicada, Universidad de Salamanca, Spain

E-mail: jeremie.torres@univ-montp2.fr

Received 14 June 2013, in final form 17 October 2013
Published 20 November 2013
Online at stacks.iop.org/SST/28/125024

**Abstract**
The potentialities of AlGaN/GaN nanochannels with broken symmetry (also called self-switching diodes) as direct and heterodyne THz detectors are analyzed. The operation of the devices in the free space heterodyne detection scheme have been measured at room temperature with RF up to 0.32 THz and explained as a result of high-frequency nonlinearities using Monte Carlo simulations. Intermediate-frequency bandwidth of 40 GHz is obtained.

(Some figures may appear in colour only in the online journal)

## 1. Introduction

At the present time, high hopes of development of solid state devices working at terahertz (THz) frequencies are connected to the use of modern electronic devices. Special attention has been paid to the development of THz Schottky diodes [1] but also to many kinds of zero-bias nonlinear devices based on III–V semiconductors for THz rectification and mixing [2–4]. Alternatively, heterojunction-based diodes have emerged [5, 6] since their planar geometry allows them to be compatible with full monolithic microwave integrated circuits (MMICs). Among these planar diodes, self-switching nanodiodes (SSDs) [7] present interesting possibilities to reach practical THz-applications since (i) they are made in only one nanolithography step by simply creating insulating trenches in a semiconductor layer, (ii) as planar devices they can be arranged as focal plane arrays and (iii) if realized with high-mobility semiconductors they can reach operation frequencies in the THz range at room temperature. Even if SSDs have been studied both numerically and experimentally as THz direct detectors [8], there is still a large margin for technology improvements to make these devices highly competitive as a solution for THz detection, both in the direct and heterodyne approaches. Indeed, heterodyne detection (widely used in radio-frequency (RF) telecommunications, imaging or astronomy) represents a significant technique for practical applications in the THz range because of its high sensitivity, its selected bandwidth of interest and its ability to recover signals on high-frequency carriers for which direct detection would otherwise be challenging. Moreover, the use of signals with carrier frequencies in the THz range opens the possibility of developing ultra-high bandwidth data transmission systems: the higher the carrier frequency, the broader is the available bandwidth for transmitting information.

The principle of heterodyne detection is that a signal carrying information (RF or THz carrier) is combined with radiation from a local oscillator (LO) operating at a frequency near that of the carrier using a device called 'mixer'. The output from the mixer is a new signal that oscillates at a frequency called the beat frequency or the intermediate frequency (IF), which is equal to the frequency difference between the LO and the original carrier. The IF is often easier to amplify and process than the original signal because it has a much lower frequency and it contains the magnitude and the phase

 

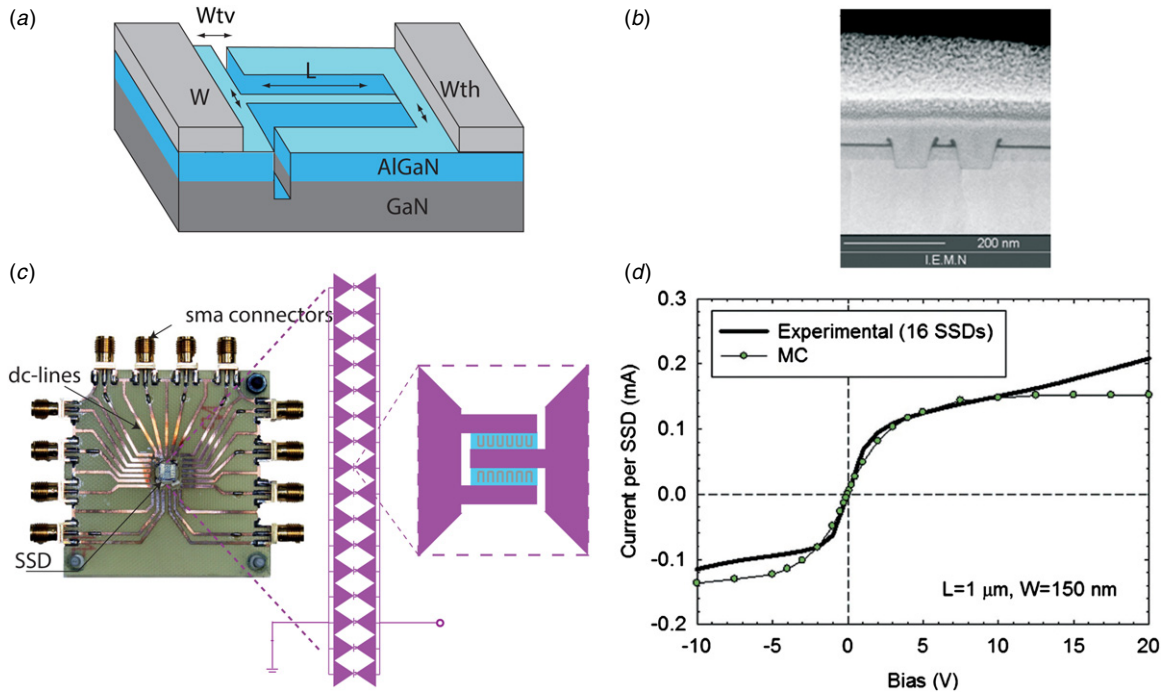


**Figure 1.** (*a*) SSD geometry, with $W$ and $L$ the channel width and length, and $W_{th}$ and $W_{tv}$ the width of the horizontal and vertical trenches respectively. (*b*) focused ion beam-cut view of the trench profile in fabricated SSDs. (*c*) Picture of the devices showing the dielectric holder with dc-line printed on it and the SMA-connectors. The scheme shows that the devices are composed of an array of 16 bow-tie antennas with 64 SSDs on each. (*d*) Current–voltage characteristic of an SSD with 1 $\mu$m length. Solid line stands for measurements, whereas points represent results from Monte Carlo simulations.

information of the THz carrier. Optical heterodyne detectors are mostly invoked when high-resolution spectroscopy is needed, while the RF superheterodyne receiver (in which the different carrier frequencies received are all converted to the same IF in order to optimize the signal amplification and filtering) is a widely used module.

However, THz heterodyne receivers typically require superconducting receivers or Schottky diode mixers [9]. The former operate at low temperatures and are very expensive and cumbersome. Even if the latter present conversion loss of ≈8 dB at 300 GHz, they are fabricated using rather complicated technological processes and designs, they require about 5 mW power to function optimally in the THz domain [10]. Moreover as vertical devices, Schottky diodes are not as compatible with a full MMIC circuit as a planar geometry would be.

In this paper, we propose to combine the high-frequency performance and planar geometry of SSDs with the heterodyne scheme to detect THz signals at room temperature. The main originality of this work consists in proposing a first implementation of GaN-SSD as THz mixer characterized by a large IF bandwidth simultaneously obtained with potentially low conversion losses.

## 2. Experimental details

### *2.1. Device fabrication*

The devices are made on an epitaxial layer consisting of 1.8 $\mu$m of undoped hexagonal GaN ([0 0 0 1] orientation) on a high resistivity Si (111) substrate (10k Ω/□), with a barrier of 23 nm of $Al_{0.3}Ga_{0.7}N$ and covered by 5 nm of SiN for passivation. Measured values of sheet carrier density $n_s$ in this epilayer are in the range 6–8 $\times 10^{12}$ cm$^2$, with a Hall mobility around 1200 cm$^2$ Vs$^{-1}$. The fabrication process starts by depositing ohmic contacts (Ti/Al/Ni/Au, with a resistance of 0.3 Ωmm) and isolation by ionic implantation ($He^+$). Then, the etching of the trenches takes place (with a PMMA resist and inductively coupled plasma chlorine based technology), and finally the top metal layer (Ti/Pt/Au) is deposited for coplanar waveguide line access. Several sizes and arrays of SSDs have been processed. A strong technological effort has been necessary in order to obtain a deep etch (45 nm) together with a small recess width (50–100 nm).

### *2.2. SSD configuration*

Even if GaN is not the optimal material for THz operation because of its lower mobility with respect to other III–V materials (e.g. InAs, InGaAs, GaAs), this work is the first step towards the development of a complete room temperature integrated THz emitter/detector system based on GaN SSDs. Indeed GaN SSDs are theoretically expected to produce also THz emission by means of Gunn oscillations up to at least 0.3 THz [11]. Here, we experimentally demonstrate their detection capabilities. Different detectors were realized with channel lengths of $L = 1$ and 2 $\mu$m. The width of the channel is $W = 150$ nm and the vertical and horizontal trenches are $W_{tv} = 100$ nm and $W_{th} = 50$ nm, respectively (see figure1(*a*)). Figure 1(*b*) is a view of the devices under test mounted on

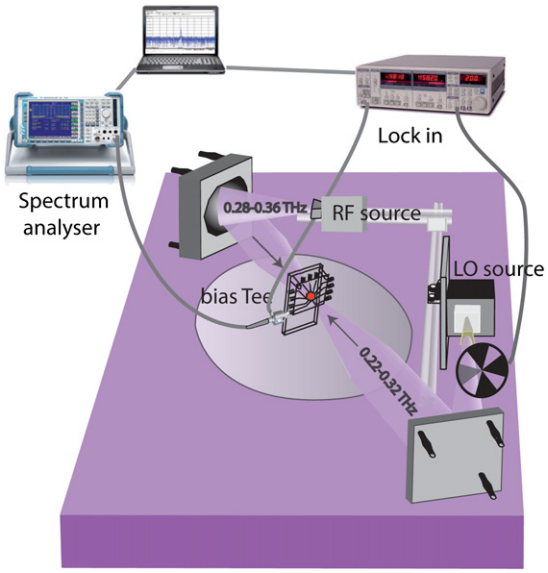


**Figure 2.** Experimental configuration. Two THz waves illuminate the device from both sides, the IF signal is measured with a spectrum analyzer, whereas a lock-in system is used on the LO signal to obtain the photoconductive response.

a FR7-holder where dc-lines are printed. In order to improve the noise equivalent power of the detectors, we designed each device as an array of 16 bow-tie antennas with 64 SSDs in parallel within each antenna, distributed in two fingers as shown in figure 1(*b*). The antennas were designed to be used with a silicon lens at the backside of the substrate. Connexions between the devices and the holder are ensured by gold-bondings, whereas connections with RF coaxial cables are made through SMA (SubMiniature version A) connectors.

### *2.3. Experimental configuration*

The THz measurements were done using two electronic sources of radiation, both based on frequency-synthesizers, whose input signal was multiplied by a factor of 27 (Figure 2). One of the sources, the LO, is tunable from 0.22 to 0.32 THz and provides a power from 0.2 to 1.8 mW depending on the frequency (average output power of about 1 mW), the other, the RF, from 0.27 to 0.36 THz provides a power from 0.6 to 0.95 mW (average output power of 0.8 mW). These two radiations are focused by two spherical mirrors on each side of the SSD, mounted on XYZ-stages. A bias-tee is connected to the SMA-connectors of the holder in order to provide the dc-bias to the devices (fed by dc voltage or current sources) and measure the IF signal produced by the mixing of the two radiations. These measurements are performed with the help of a spectrum analyzer between ≈dc and 40 GHz. Also direct detection measurements (photoresponse) were done by using only the LO source. The beam was mechanically chopped at 217 Hz for lock-in detection.

### *2.4. Monte Carlo simulations*

In order to understand the physical mechanisms and optimize the performances of the devices, a semi-classical Monte

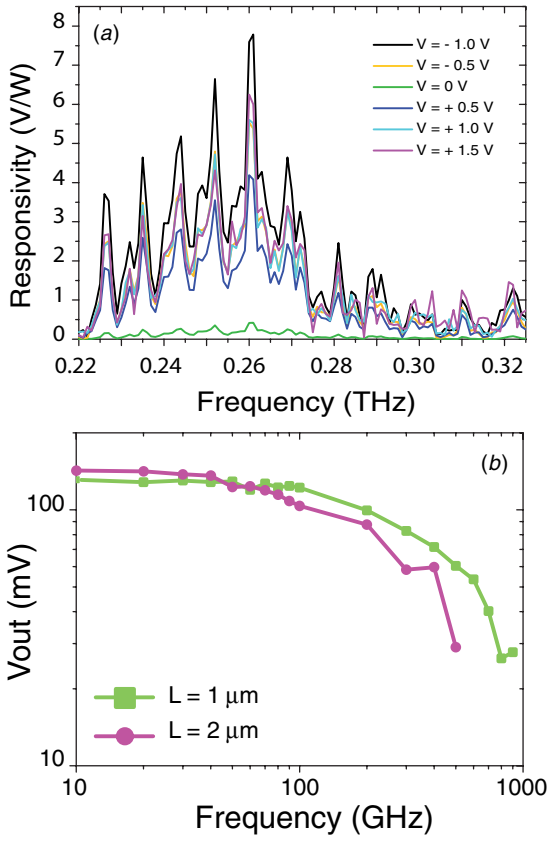


**Figure 3.** (*a*) Responsivity as a function of the frequency of the incident THz radiation measured at $T = 300$ K for the SSD with $L = 1$ $\mu$m for different applied voltages (in both direct and reverse bias conditions). (*b*) Mean voltage through a SSD versus the frequency calculated by Monte Carlo simulations for 1 and 2 $\mu$m long devices.

Carlo (MC) simulation self-consistently coupled with a Poisson solver is used [12]. We have performed 'top-view' 2D simulations where only the channel is modeled and the influence of the fixed charges present in the layer structure (essentially negative charges at the top surface of AlGaN and positive piezoelectric charges at the AlGaN/GaN heterojunction) is accounted for by means of a 'virtual' background doping $N_{Db}$. In order to include the effect of the depletion originated by charges present in surface states at the semi-conductor–dielectric boundaries of the insulated trenches, a negative charge density $\sigma$ is considered, whose value is updated self-consistently with the carrier dynamics near the interface during the simulation, so that the surface charge at a given position is adapted to the carrier density in the nearby region. The good agreement between the dc experimental measurements and the MC simulations of the $I$–$V$ curve of a single SSD with 1 $\mu$m length is shown in figure 1(*d*).

## 3. Results and discussion

### *3.1. Photoresponse results*

Figure 3(*a*) shows the photoconductive response versus excitation frequency at room temperature for different applied

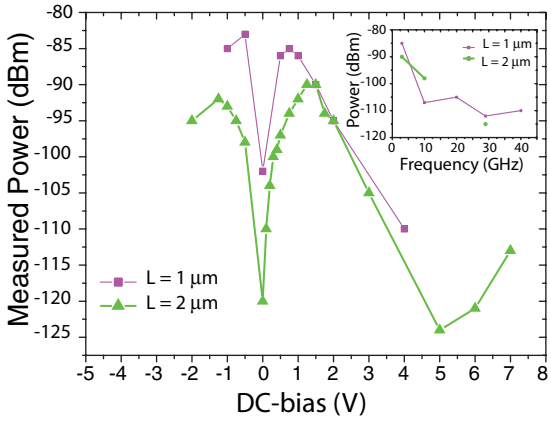


**Figure 4.** Measured power of the IF signal versus applied voltage for the array of SSDs with 2 $\mu$m length at an RF frequency of 0.3 THz and an IF frequency of 3 GHz. The inset shows its frequency dependence at the dc bias providing the maximum IF power for both 1 $\mu$m- and 2 $\mu$m-long SSDs.

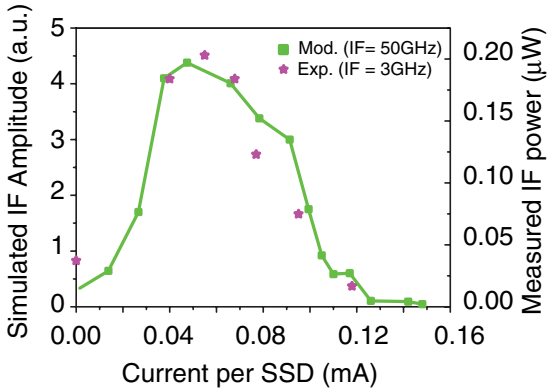


**Figure 5.** Monte Carlo simulation of the IF amplitude at 50 GHz versus the bias current per SSD with 1 $\mu$m length compared with the experimental results obtained at 3 GHz.

voltages. At zero bias, the measurements provide small values for the responsivity with resonant features and a cut-off frequency at ≈0.3 THz. Since no Si-lens was used in our experiments, the bow-tie antennas are probably irrelevant in determining this cut-off. We believe that this behavior is mainly associated with the presence of the bonding-wires which act as unintentional additional antennas [13]. Consequently, the resonant features observed in the spectrum of figure 3(*a*), can be explained by the formation of standing-waves in these wires [14].

Indeed, the MC calculations shown in figure 3(*b*) demonstrate that this cut-off frequency is not due to intrinsic properties of the GaN-based devices, since the amplitude of the mean voltage obtained as a result of rectification in 1 $\mu$m- and 2 $\mu$m-long devices has cut-off frequencies around 0.9 THz and 0.45 THz, respectively. The poor efficiency of the coupling of the free space radiation to the devices (partially due to the absence of the Si-lens at the backside of the substrate) is confirmed by the fact that measurements of similar devices connected with coplanar wave lines and characterized making use of a vector network analyzer at frequencies up to 0.32 THz provide much higher values for the responsivity [15].

In order to improve the performance of the devices, different dc biases were applied to the SSD array (while the power of the THz beam was kept constant), resulting in an increase by a factor of ≈15, reaching a maximum of ≈8 V/W at $V = -1$ V. This behavior reflects the nonlinearity of the device *I*–*V* characteristic shown in figure 1(*d*): the highest responsivities are found at the biases corresponding to the corner voltages of the *I*–*V* curve, where its nonlinearity is maximum.

### *3.2. Mixing results*

Moving to mixing experiments, figure 4 shows the power of the IF signal measured for both the 1 $\mu$m- and 2 $\mu$m-long devices versus the applied dc voltage at the IF frequency of 3 GHz. Even if the present experimental configuration and devices are not optimized, the dynamic range, measured at the spectrum analyzer with a resolution bandwidth of 2 Hz, ranges between 50 and 65 dB; that is comparable to systems found in the literature at room temperature [9]. In those experiments, the noise floor is at −135 dBm. One can note that this dynamic range is lower than, for example, that of commercially available Schottky diodes (of around 100 dB, see for example [16]), but in that case the devices are optimized for a central frequency (for example 300 GHz) with an IF bandwidth between 5 MHz and 1 GHz. Moreover, the conversion losses of the full sample (SSDs, bondings, holder and connection) are approximately 80 dB. They have been determined from the ratio of the IF measured power (−82 dBm, in the best bias conditions) to the incoming radiation power (−2 dBm, measured at the output of the RF source at the frequency of 0.3 THz).

As expected, the bias dependence of the output voltage observed in figure 4 shows a maximum between 1.5 V and 2.0 V which reflects the nonlinearity of the device *I*–*V* characteristics (very similar to those presented in figure 1(*a*)). This result is consistent with the estimation based on the calculation of the nonlinear curvature coefficient [17]. This relationship is well reproduced by the MC simulations, whose comparison with the experiments for the SSDs with 1 $\mu$m length is plotted in figure 5. In the case of MC simulations the amplitude obtained for the IF signal is constant when its frequency is below 0.1 THz, thus evidencing that the frequency dependent response obtained in the measurements is not due to the intrinsic behavior of the SSDs. This is also confirmed by the results shown in the inset of figure 4, presenting the maximum IF amplitude versus its frequency for both the 1 $\mu$m- and 2 $\mu$m-long devices, which strongly depends on the channel length.

## 4. Discussion

Given that the response of our system is limited by extrinsic elements, mainly the connections from SSDs to the equipments, we have tried to characterize the main sources of losses.

- Losses due to coaxial and bias-tee connections to the spectrum analyzer have been measured with the help of a network analyzer (about 1.1 to 4.2 dB from 3 to 40 GHz).

- Losses due to the SMA connectors and dc lines on the dielectric holder where the samples are mounted have been simulated by CST microwave studio (about 5 to 17 dB from 3 to 40 GHz).

Consequently, the corrected conversion losses can be estimated as $80 - (17 + 4.2) \approx 59$ dB. However, this value does not represent the intrinsic conversion losses of the SSDs. Indeed the losses due to antennas and bondings-wires, whose values are difficult to estimate, should also be taken into account.

The previous results demonstrate the good performance of SSDs acting as a heterodyne receiver system, which can be significantly improved simply by optimizing (i) the antenna design and the coupling between the RF and LO signals to the SSD by the help of Si-lens and (ii) the external connections (mainly by improving the access losses and the large impedance mismatch with our highly resistive devices (35 kΩ for one SSD)), thus being possible to envisage the fabrication of a heterodyne detection system with an IF signal at much higher frequencies, above 100 GHz, paving the way for applications such as ultra-high data-rate wireless transmission. Additionally, the intrinsic design of the SSD can also be improved by (i) decreasing the channel length and (ii) using high-mobility semiconductors such as InGaAs or InAs, which raises the intrinsic cut-off frequency of the SSDs [18], thus making possible the increase of both the frequency of the carrier signals and the bandwidth of the heterodyne receiver.

## 5. Conclusion

In summary, we have demonstrated that self-switching nanodiodes (SSDs) can be employed as mixers for sub-THz heterodyne detection. In this first implementation, conversion losses of ≈59 dB simultaneously with an intermediate frequency (IF) bandwidth of at least 40 GHz have been obtained. Even if these values are not yet competitive with state-of-the-art commercial systems (e.g. Schottky diodes all-in-package and guided configuration: conversion loss ⩽8 dB and IF bandwidth ⩽30 GHz), there is still a large margin for the improvement of design and technology. Beyond the proper choice of the connective elements (taking into account impedance matching, IF signal bandwidth,. . .) as well as the integration with adequate waveguides and optical coupling optimization (using silicon lens, sample packaging,. . .), the scaling of the geometry of the SSDs and the use of high electron mobility materials can boost the bandwidth of this type of system. In fact, GaAs based SSDs have already demonstrated room temperature 1.5 THz detection [8], paving the way to achieve heterodyne detection up to at least 2 THz. In addition, further optimizations include a careful design of the channel length and geometry (channel shape, vertical trenches width, etc) in order to increase the amplitude of the IF signal, and even take advantage of an enhanced response due to the plasma resonances and intrinsic noise optimization. Furthermore, the planar geometry and the ease of fabrication of these nanodiodes makes them highly competitive in the prospect of a new generation of terahertz detectors.

## Acknowledgments

This work has been partially supported by the European Commission through the ROOTHz Project ICT-2009-243845, by the Direccion General de Investigacion (MICINN) and the Consejeria de Educacion de la Junta de Castilla y Leon through Projects TEC 2010-15413 and SA183A12-1, respectively. Support by TERALAB Montpellier is also acknowledged.

## References

[1] Cojocari O, Mottet B, Rodriguez-Girones M, Biber S, Marchand L, Schmidt L-P and Hartnagel H L 2004 A new structural approach for uniform sub-micrometer anode metallization of planar thz schottky components *Semicond. Sci. Technol.* **19** 537–42

[2] Semenov A, Cojocari O, Hübers H-W, Song F, Klushin A and Müller A-S 2010 Application of zero-bias quasi-optical schottky-diode detectors for monitoring short-pulse and weak terahertz radiation *IEEE Electron Device Lett.* **31** 674

[3] Young A C, Zimmerman J D, Brown E R and Gossard A C 2005 Semimetal-semiconductor rectifiers for sensitive room-temperature microwave detectors *Appl. Phys. Lett.* **87** 163506

[4] Casini R, Di Gaspare A, Giovine E, Notargiacomo A, Ortolani M and Foglietti V 2011 Three-dimensional shaping of sub-micron gaas Schottky junctions for zero-bias terahertz rectification *Appl. Phys. Lett.* **99** 263505

[5] Seliuta D *et al* 2004 Detection of terahertz/sub-terahertz radiation by asymmetrically-shaped 2DEG layers *Electron. Lett.* **40** 631

[6] Xu K Y, Lu X F, Song A M and Wang G 2008 Enhanced terahertz detection by localized surface plasma oscillations in a nanoscale unipolar diode *J. Appl. Phys.* **103** 113708

[7] Song A M, Missous M, Omling P, Peaker A R, Samuelson L and Seifert W 2003 Unidirectional electron flow in a nanometer-scale semiconductor channel: a self-switching device *Appl. Phys. Lett.* **83** 1881–3

[8] Balocco C, Kasjoo S R, Lu X F, Zhang L Q, Alimi Y, Winnerl S and Song A M 2011 Room-temperature operation of a unipolar nanodiode at terahertz frequencies *Appl. Phys. Lett.* **98** 223501

[9] Siegel P H and Dengler R J 2007 Terahertz heterodyne imaging parts II *Int. J. Infrared Millim. Waves* **5** 631–54

[10] Wanke M C, Young E W, Nordquist C D, Cich M J, Grine A D, Fuller C T, Reno J L and Lee M 2010 Monolithically integrated solid-state terahertz transceivers *Nature Photon.* **4** 565–9

[11] Iñiguez de-la Torre A, Iniguez de-la Torre I, Mateos J, Gonzalez T, Sangare P, Faucher M, Grimbert B, Brandli V, Ducournau G and Gaquiere C 2012 Searching for THz Gunn oscillations in GaN planar nanodiodes *J. Appl. Phys.* **111** 113705

[12] Mateos J, Vasallo B G, Pardo D and Gonzalez T 2005 Operation and high-frequency performance of nanoscale unipolar rectifying diode *Appl. Phys. Lett.* **86** 212103

[13] Ortolani M *et al* 2009 Study of the coupling of terahertz radiation to heterostructure transistors with a free electron laser source *J. Infrared Millim. Terahertz Waves* **30** 1362–73

[14] Jeon T-I, Zhang J and Grischkowsky D 2005 THz Sommerfeld wave propagation on a single metal wire sommerfeld wave

propagation on a single metal wire *Appl. Phys. Lett.* **86** 161904

[15] Sangare P *et al* 2013 Experimental demonstration of direct terahertz detection at room-temperature in algan/gan asymmetric nanochannels *J. Appl. Phys.* **113** 034305

[16] Radiometer Physics Gmbh 2011 *Product Data Sheet* (Meckenheim: Radiometer Physics Gmbh)

[17] Zhou Q, Wong K-Y, Chen W and Chen K J 2010 Wide-dynamic-range zero-bias microwave detector using AlGaN/GaN heterojunction field-effect diode *IEEE Microw. Wirel. Compon. Lett.* **20** 277–9

[18] Iñiguez-de-la-Torre I, Gonzalez T, Rodilla H, Vasallo B G and Mateos J 2011 *Applications of Monte Carlo Method in Science and Engineering* vol 33 ed S Mordechai (Rijeka: InTech)